

Amination of Polymeric Braid Structures to Improve Tendon Healing: An Experimental Comparison

Tânia Peixoto, Daniel Silva, Miguel Rodrigues, Miguel Neto, Rui Silva, Maria C. Paiva, Liliana Grenho, Maria Helena Fernandes, and Maria A. Lopes*


Several polymers are researched for tendon repair as polyethylene terephthalate (PET) and polylactic acid (PLA). These are biocompatible and useful in scaffolding repair though with minimal success due to long-term failure. There is a need to improve such scaffolds' design and physical–chemical nature. This work concerns surface functionalization of polymeric braids (PET and PLA) that fulfill the high mechanical demands of tissues such as tendons. The functionalization aims to incorporate amine groups in the braids' surface, improve cell adhesion, and consequently, the poor healing rate of these tissues and the biointegration of the braids. Two approaches are compared: the direct application of NH_3 plasma and the surface grafting of EDA after O_2 plasma activation. X-ray photoelectron spectroscopy (XPS) shows that amine groups are effectively introduced onto the samples' surfaces. Besides, the plasma parameters chosen do not compromise the topography and tensile behavior of the braids. Resazurin assay and scanning electron microscopy show that the NH_3 treatment improves cell–biomaterial interaction as improved cell adhesion and proliferation are observed. Both approaches are safe for biomedical applications. The NH_3 plasma approach is more environmentally friendly, faster, and easier to scale-up, showing potential for application in the final hybrid medical device.

1. Introduction

Tendons are connective tissues that bind muscle to bone, with great ability to transmit forces, withstand tension, and release stored energy, providing strength and the necessary stability for human posture and locomotion.^[1–3] These tissues are constantly under repeated motions and degeneration, presenting high vulnerability to injury. Surgical intervention is often needed because tendons show limited self-healing capacity.^[2,4] Traditional reconstruction techniques based on sutures or autografts/allografts present associated disadvantages, often failing to accomplish an adequate long-term solution.^[2,5] Synthetic grafts can be designed to present similar mechanical properties and dimensions to the native tissues.^[2] However, these synthetic prostheses have been mainly produced from non-degradable polymers. Commonly reported problems include insufficient long-term mechanical durability and lack of biointegration capacity to enable appropriate biological tissue ingrowth into their structure.^[5,6]

T. Peixoto, D. Silva, M. Rodrigues, M. A. Lopes
 REQUIMTE-LAQV, Departamento de Engenharia Metalúrgica e
 Materiais, Faculdade de Engenharia
 Universidade do Porto
 Rua Dr. Roberto Frias, Porto 4200-465, Portugal
 E-mail: malopes@fe.up.pt

T. Peixoto, M. C. Paiva
 Instituto de Polímeros e Compósitos, Departamento de Engenharia de
 Polímeros
 Universidade do Minho
 Guimarães 4800-058, Portugal
 M. Neto, R. Silva
 CICECO, Departamento de Engenharia de Materiais e Cerâmica
 Universidade de Aveiro
 Aveiro 3810-193, Portugal
 L. Grenho, M. H. Fernandes
 Laboratory for Bone Metabolism and Regeneration, Faculdade de
 Medicina Dentária
 Universidade do Porto
 Rua Dr. Manuel Pereira da Silva, Porto 4200-393, Portugal
 L. Grenho, M. H. Fernandes
 LAQV/REQUIMTE
 Universidade do Porto
 Porto 4160-007, Portugal

 The ORCID identification number(s) for the author(s) of this article can be found under <https://doi.org/10.1002/mame.202200426>

© 2022 The Authors. Macromolecular Materials and Engineering published by Wiley-VCH GmbH. This is an open access article under the terms of the Creative Commons Attribution License, which permits use, distribution and reproduction in any medium, provided the original work is properly cited.

DOI: 10.1002/mame.202200426

To address these shortcomings, fibrous textile structures as tissue scaffolds have been popular targets due to their versatility, morphological similarity to the natural extracellular matrix (ECM), and mechanical anisotropy to resemble biological tissues.^[7] An innovative medical device produced from hybrid textile braids based on PET and PLA yarns was developed in previous work.^[8,9] This device mimics the hierarchical morphological features and fulfills the high mechanical demands of tissues such as tendons and ligaments. The superior tensile properties and creep/fatigue resistance of PET allow this medical device to provide adequate physical support for cell proliferation and differentiation. At the same time, PLA's degradability will mainly enhance tissue growth and device biointegration in the long term.

Metabolically, after an injury, tendon healing occurs in the form of a slow process that might take months or years.^[10] PLA was chosen as an appropriate material because of its long degradation time (months to a few years, depending on crystallinity and molecular weight).^[11] The device must maintain its functionalities during the early phases of healing and withstand the required load before degrading and then being replaced by new tissue. At this point, cells from the surrounding native environment should have penetrated the device's extremities, which are sutured to the original tissue. However, the hypocellularity characteristic of tendons and ligaments limits their healing capacity, even after repair.^[12] To further optimize the ability of this device to enhance tendon healing, various surface treatments may be applied to alter the chemical behavior of polymer surfaces to enhance biocompatibility and increase cell migration, adhesion, and proliferation into the device, which along with the degradation, will contribute to the success of the implant in the long term.

The use of plasmas, in particular, to alter the surfaces of biomaterials has been beneficial to improve biocompatibility or biological activity on the surface.^[13,14] In fact, the wide range of biomaterials-based plasma treatments is reported to have a beneficial role on such materials, from cell proliferation to lab-on-a-chip development.^[15,16] Plasma technologies can be a low-cost approach that provide a wide range of surface functionalities. As a result, it is being successfully used to enhance polymers' surface properties, such as roughness, hydrophilicity, and surface chemistry.^[13,17]

Plasma treatments that produce surfaces containing amine, carboxy, or hydroxy groups, have been popular for biomedical applications.^[18] These parameters should be tuned so that thermal heating and/or excessive plasma etching do not cause severe structural damage and/or roughening of the polymer.^[19] Thus, choosing an appropriate surface modification without compromising the fibrous structures' surface and mechanical properties can be challenging.^[20]

Within this framework, the authors aimed to alter the surface properties of the previously developed synthetic textile hybrid braids to positively affect the interactions between cells and the fibers. Two approaches for the surface functionalization of these novel hybrid braids are compared: the direct application of reactive NH₃ plasma treatment and the surface grafting of EDA after O₂ plasma activation to produce in situ amine function groups. Both approaches are scalable for industrial application; although, the NH₃ approach, being solvent free, is more environmentally friendly. The braids were subjected to morphological, chemical,

and mechanical characterization. Cellular viability was also evaluated based on the most promising treatments.

2. Experimental Section

2.1. Materials

PET yarn (≈ 192 filaments, 1100 dtex) was obtained from Sarla Europe (Portugal). PLA yarn (≈ 108 filaments, 1100 dtex) was purchased from Senbis Polymer Innovations (The Netherlands). Ethylenediamine (EDA) (99%) was obtained from Alfa Aesar (Thermo Fisher (Kandel) GmbH, Germany).

2.2. Methods

2.2.1. Braids Production

The braids were produced as described in a previous work by the same research team.^[8] Briefly, a vertical braiding machine with 16 carriers (Trenz Export Sa, Spain) was used to produce PET and PLA braids based on those yarns, using 16 yarns and a take-up rate of $\approx 3.96 \text{ cm s}^{-1}$.

2.2.2. Plasma Treatments

The produced braids were exposed to different activation treatments in an Emitech K1050X solid-state RF plasma barrel reactor. Different plasma treatments were performed using O₂ and NH₃ gases, with 99.9995% and 99.999% purity (Air Liquid), respectively. The reactive plasmas were produced with a maximum 100 W power @13.56 MHz. First, the functionalization parameters were optimized by studying the effect of plasma pressure and exposure time on PET (Phase 1). Then, the selected most promising treatment parameters were applied to PLA (Phase 2). **Table 1** summarizes the plasma treatment parameters used.

Immediately after each O₂ plasma treatment, PET and PLA samples were immersed in an EDA solution, using water as solvent (50% v/v), at 50 °C and 20 min. After immersion, the samples were removed from the solutions and rinsed in distilled water.

2.2.3. Characterization

Physico-Chemical and Mechanical Characterization: The effectiveness of the variation of O₂EDA and NH₃ functionalization parameters was evaluated by the Orange II dye method by quantifying amino groups in the PET samples' surface. The samples, measuring $\approx 5 \text{ cm}$ in length and $\approx 3 \text{ mm}$ in diameter, were immersed in 20 mL of dye acidic solution (14 mg mL^{-1}) (pH 3) and incubated for 1 h at 40 °C and 150 rpm. After that, the samples were washed with an acidic solution (pH 3) to remove the non-reacted dye. After air-drying, the samples were immersed in 5 mL of an alkaline solution (pH 12) and incubated for 15 min at room temperature and 150 rpm. The absorbance of the solution was determined at a wavelength of 485 nm in a UV spectrophotometer (UV-1800 Shimadzu, Japan), using quartz cells with a 10 mm

Table 1. Plasma treatment parameters: reactive gas, plasma pressure, and exposure time, during functionalization of the PET and PLA braids.

Sample name	Reactive gas	Plasma Pressure [mbar]	Exposure time [min]
Phase 1: Optimization of functionalization conditions in PET braids			
PET_NH ₃ _7.5_3	NH ₃	7.5 × 10 ⁻²	3
PET_NH ₃ _7.5_8			8
PET_NH ₃ _7.5_12			12
PET_NH ₃ _7.5_20			20
PET_NH ₃ _1_8		1.1 × 10 ⁻¹	8
PET_NH ₃ _1_12			12
PET_O ₂ EDA_7.5_3	O ₂	7.5 × 10 ⁻²	3
PET_O ₂ EDA_7.5_8			8
PET_O ₂ EDA_7.5_12			12
PET_O ₂ EDA_7.5_20			20
PET_O ₂ EDA_1_8		1.1 × 10 ⁻¹	8
PET_O ₂ EDA_1_12			12
Phase 2: Functionalization of PLA braids			
PLA_NH ₃ _7.5_12	NH ₃	7.5 × 10 ⁻²	12
PLA_O ₂ EDA_7.5_12	O ₂	7.5 × 10 ⁻²	12

pathlength. After optimizing the functionalization parameters, this method was also used to quantify amino groups in the PLA braids based on the selected treatment conditions. This study was repeated one month after functionalization to assess the stability of the amino groups in both PLA and PET braids.

The PET and PLA braids were stained with fuchsin acid 0.5% in pH 3 buffer solution for 90 min at room temperature under stirring to assess the distribution of amine-based groups throughout the samples. The stained samples were rinsed in a pH 3 buffer solution to remove the non-linked dye.

The surface chemistry was assessed by X-ray photoelectron spectroscopy (XPS) using a Kratos Axis Ultra HSA spectrometer. A monochromatic Al K_α source operating at 15 kV (90 W) with a pass energy of 40 eV for regions of interest and 160 eV for the overall surveys was used for the study. CasaXPS software was used to analyze the information. Curve fitting was done with a linear background and a GL^[30] lineshape. The binding energy was calculated using the C1 S of hydrocarbon at 285.0 eV.

The surface morphology of the braids was studied using scanning electron microscopy (SEM) using a FEI Quanta 400FEG microscope (ThermoFisher Scientific, USA).

The tensile mechanical characteristics were measured using a Lloyd Instruments LR 30K equipment with a 2.5 kN load cell. A gauge length of 235 mm and a crosshead speed of 8.5 mm s⁻¹ were used.

In Vitro Biological Characterization: As the PET yarns represent the most significant percentage of the composition of the hybrid device, in vitro studies were conducted on PET braids to evaluate and compare the effect of both functionalization approaches on cellular viability. The braids were cut into samples of 2 cm in length (≈3 mm in diameter). Human dermal fibroblasts (Coriell Institute) were cultured in alpha-minimal essential medium (α-MEM) supplemented with 10% (V/V) fetal bovine serum (FBS), 100 U mL⁻¹ penicillin, 100 μg mL⁻¹ streptomycin, and 0.25 μg mL⁻¹ amphotericin B (all reagents from

Gibco). Cells were seeded at two different locations on the surface of the samples (untreated PET, PET_O₂EDA_7.5_12 and PET_NH₃_7.5_12) at 2 × 10⁴ cells per sample. The plates were further incubated for up to 21 days at 37 °C, in a 5% CO₂ humidified atmosphere.

Metabolic activity was assessed by resazurin assay. After medium removal, the seeded materials were incubated at each time point with a fresh medium containing 10% resazurin (0.1 mg mL⁻¹, Sigma–Aldrich). The plates were incubated for 3 h at 37 °C in a humidified atmosphere with 5% CO₂. In a microplate reader (Synergy HT, Biotek), the fluorescence (excitation: 530 nm; emission: 590 nm) was measured. Relative fluorescence units (RFUs) were used to display the results.

Cell morphology was observed by SEM using a FEI Quanta 400FEG microscope (ThermoFisher Scientific, USA). Previously, samples were rinsed in PBS and fixed for 15 min with 1.5% (V/V) glutaraldehyde in sodium cacodylate buffer (pH 7.3). After that, samples were dehydrated with increasing ethanol solutions and critical point dried (CPD 7501, Polaron Range). Finally, samples were sputter-coated (SPI-Module) with a thin gold/palladium film.

2.3. Statistical Analysis

The data is presented as a mean value with a standard deviation. The one-way ANOVA test was used in the statistical analysis and *t*-tests in SigmaStat software were used to examine group differences. At a *p* < 0.05 threshold of significance, differences were deemed statistically different.

3. Results and Discussion

An innovative medical device produced from hybrid textile braids based on PET and PLA yarns was developed in a previous work.^[8,9] The designed device presents a core–shell architecture (several hybrid braids surrounded by an exterior shell of braided PET yarns) that mimics the hierarchical morphological features and fulfills the high mechanical demands of tissues such as tendons and ligaments. During the first phase of the repair process, the non-degradable component (PET) protects the cells and newly formed tissue from excessive strains by withstanding physiological loads and providing mechanical support, allowing the body's natural healing process to take place. The degradable component (PLA) would enable gradual load exposure and new tissue ingrowth in later phases, enabling device integration with surrounding host tissues while preserving biological repair. Nevertheless, due to the poor and slow healing rate of these tissues, along with their hypocellularity, the biofunctionality of the device should be improved to allow for a faster cell migration into the device and, consequently, adhesion and proliferation, to increase the rate of new tissue ingrowth.

Hybrid braids with a higher PET to PLA ratio demonstrated suitable mechanical properties for the intended purpose.^[8,9] As such, the primary purpose of this work was to surface modify the PET yarns, which are present in higher number in the hybrid medical device. PLA was also functionalized to evaluate the impact of the surface modification process on the performance of the hybrid medical device.

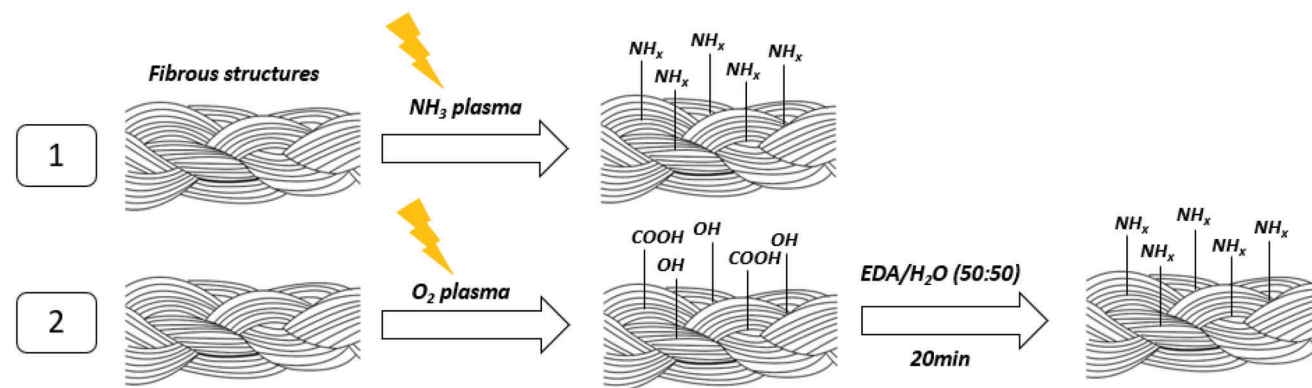


Figure 1. Schematics of the functionalization approaches and expected results used in this study.

The present work explores two approaches to overcome the biological inertness of the surface of this synthetic medical device to improve cell interaction and, consequently, tendon healing.

Synthetic polymers have been the material of choice for these applications due to their availability and simpler production.^[21,22] They often present a hydrophobic nature with low surface energy, leading to poor wettability, and limited cellular adhesion and growth.^[17] These properties play an important role in the success of a scaffold because they affect cell–material interactions^[23] and can profoundly impact the repair process.

Two approaches for surface functionalization were compared regarding their effect on the functionalization, morphological, and tensile properties of the braids, and cellular viability: the direct application of reactive NH_3 plasma treatment and the surface grafting of EDA after O_2 plasma activation, to create nitrogen-containing functions in situ (**Figure 1**). NH_x species may be generated in NH_3 plasma either by directly dissociating NH_3 molecules or by recombining N and H species generated in the plasma.^[24] The second method involves reacting an amine with an ester group, which results in chain scission and amide production at the reaction site.^[25] In the present work, a diamine was used, namely EDA. The chain scission process consumes one of the amine groups, which reacts with the polymer to form an amide group, leaving the remaining amine group free, and linked to the polyester structure,^[25] available for biological interactions. Before immersion in EDA, the polymer substrates are exposed to O_2 plasma treatment to increase surface hydrophilicity, improve the contact with the EDA in solution, and create reaction points to anchor EDA molecules.

Both approaches can be considered safe for biomedical applications and easily scaled up. Nevertheless, the first approach is faster, being a dry process that avoids liquid waste, resulting in an environmentally friendly approach.^[13]

3.1. Physico-Chemical and Mechanical Characterization

In the first phase of the study, the PET functionalization parameters, namely plasma pressure and exposure time, were varied. The goal was to evaluate the impact of these parameters' variation on the effectiveness of the functionalization. A colorimetric assay based on Orange II was used to quantitatively evaluate the extent

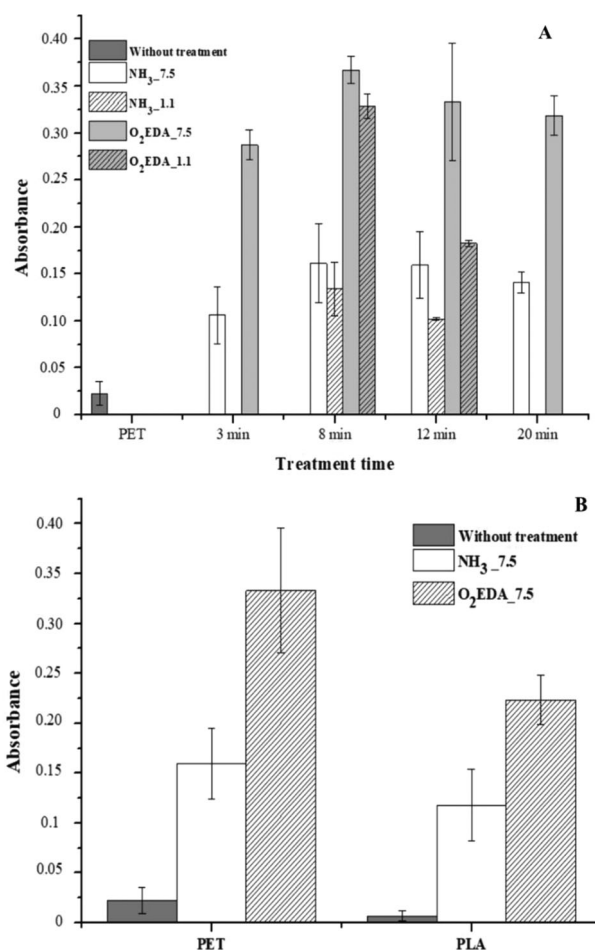


Figure 2. Orange II results: a) optimization of treatment parameters in PET braids and b) comparison between PET and PLA braids after functionalization with the most promising treatments.

of amino group grafting resulting from both approaches because it is a commonly used dye for amino group density quantification (primary, secondary, and tertiary amines).^[26,27] **Figure 2a** presents the acid orange absorbance values after functionalizing the PET braids using the different conditions.

A nonsignificant Orange II concentration was obtained for pristine PET, suggesting that nonspecific interactions between PET and the dye were negligible. It is possible to observe that the highest absorbance levels correspond to the samples treated with O₂ plasma and EDA. The PET_O₂EDA_7.5_3 sample's absorbance was significantly different from the PET_O₂EDA_7.5_8 ($p < 0.05$) but no significant differences were found among the samples treated for 8, 12, and 20 min. The effect of the pressure of the O₂ plasma was also accessed by increasing it to 1.1×10^{-1} mbar for two treatment times, 8 and 12 min. In both cases, increasing plasma pressure resulted in an absorbance decrease ($p < 0.05$) but was more accentuated for the longer treatment period of 12 min. Regarding the NH₃ treated samples, the PET_NH₃_7.5_3 sample's absorbance was significantly different from the PET_NH₃_7.5_8 and PET_NH₃_7.5_12 ($p < 0.05$) but no significant differences were found among the samples treated for 8, 12, and 20 min. The effect of the pressure of the NH₃ plasma was also accessed by increasing it to 1.1×10^{-1} mbar for the same two treatment times, 8 and 12 min. While no significant difference was noted for the samples treated for 8 min, increasing plasma pressure in the 12 min treated samples resulted in an absorbance decrease ($p < 0.05$), as observed for the O₂ EDA treated samples.

It is possible that by increasing plasma pressure, the modification induced structural damage and/or roughening of the polymer fibers due to the combination of thermal heating and etching.^[19] This fact may also explain why for this plasma pressure, the absorbance decrease was more accentuated for the exposure time of 12 min because the substrate was exposed for a longer period to possible damage.

As a result of this functionalization optimization, the lowest plasma pressure tested was chosen for the next phase because it demonstrated a better functionalization ability in both plasma approaches. Regarding treatment time, 12 min appeared to be a good equilibrium between the highest treatment times (8, 12, and 20 min). These conditions (plasma pressure of 7.5×10^{-2} mbar and 12 min) were selected for the next phase (PLA functionalization).

Figure 2b presents the absorbance values after functionalizing the PLA braids using the previously selected plasma treatments. A nonsignificant Orange II concentration was obtained for neat PLA, similar to what was observed for the neat PET sample. It is possible to observe that the highest absorbance levels correspond to the samples treated with O₂ plasma and EDA but are lower than the ones registered for PET ($p < 0.05$). On the other hand, PLA_NH₃_7.5_12 demonstrated a significantly lower absorbance than the other treatment. In this case, no significant differences were found between PET and PLA.

The Orange II method for amino group density quantification was performed one month after functionalization to assess the stability of the amino groups in both PLA and PET braids. This method was conducted first at pH = 3 to ensure the reaction between the dye and the amino groups. After the reaction took place and the non-reactive species were washed away, the samples were subjected to pH = 12 to reverse the process and decouple the amino groups for quantification. **Figure 3** shows the obtained acid orange absorbance values one month after functionalizing the PET and PLA braids using both approaches. No statistical differences were found between the two time points for PET and PLA. Thus, it can be concluded that both treatments

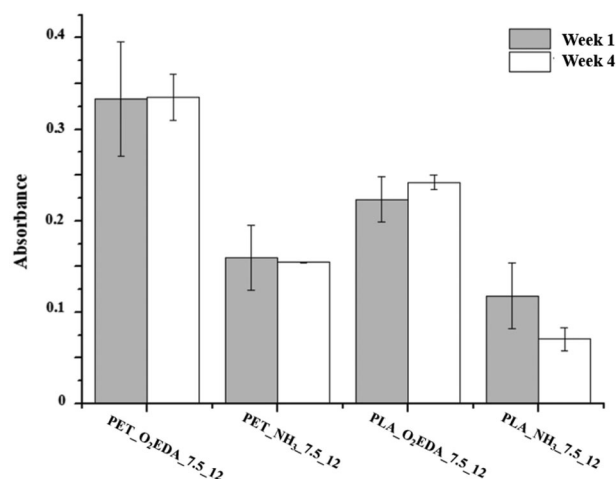


Figure 3. Orange II results one month after functionalization.

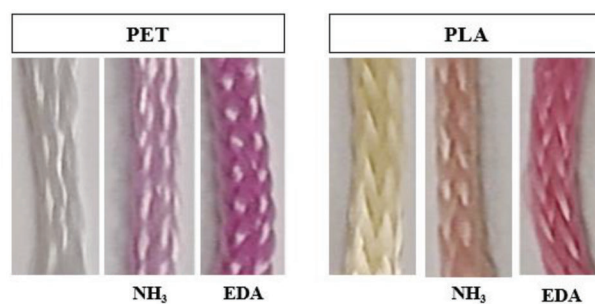


Figure 4. PET and PLA braids after fuchsin acid staining.

are stable during this period, which is relevant for evaluating the shelf life of the final medical device.

The previously selected conditions, namely PET_NH₃_7.5_12, PET_O₂EDA_7.5_12 and PLA_NH₃_7.5_12, PLA_O₂EDA_7.5_12 were stained with fuchsin acid dye (**Figure 4**) to qualitatively evaluate the amine groups distribution throughout the braids. This dye has been successfully used to detect amine groups at an acidic pH.^[25] This compound is a sodium sulfonate derivative of fuchsin, which reacts with primary amines at an acidic pH, resulting in a purple color that gets darker with increasing concentration of primary amine groups.

After staining, the untreated PET and PLA braids remained uncolored, as expected. At the same time, the NH₃ and O₂EDA treated samples became purple, indicating a homogeneous distribution of amine-based groups throughout the samples.

Surface chemical modifications induced by the studied treatments were determined by XPS analysis. This method allows obtaining more detailed information about the type of reaction that took place and resulting bonds/elements, which the previous methods had not clarified. The chemical bonds and binding energy (eV) of PET samples, along with atomic concentration, are shown in **Table 2**. **Figure 5** shows the survey spectra of PET surface before and after both treatments, along with the C1s (Figure 5a), O1s, and N1s high-resolution spectra (Figure 5b).

As the nitrogen was attached to the PET filaments' surface, the new N 1s peak rose dramatically after NH₃ treatment, as seen in the survey spectra.^[28]

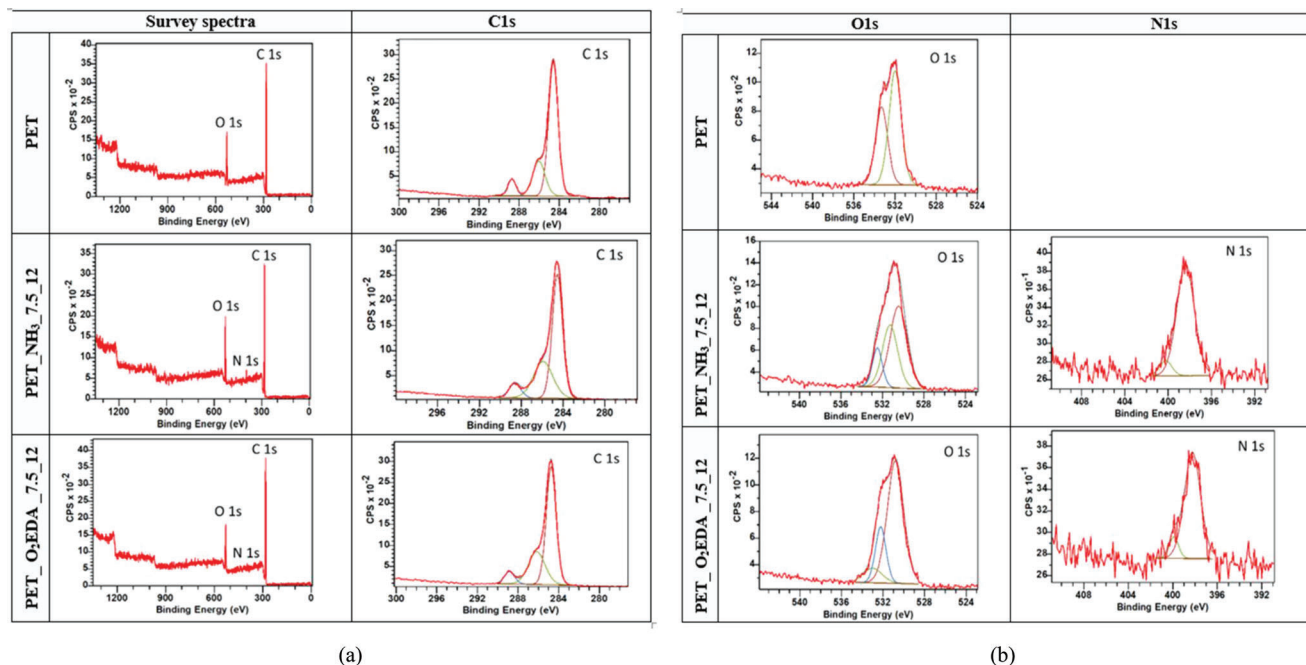


Figure 5. a) XPS overview and detailed spectra (C1s) of untreated and treated PET braids, b) detailed spectra (O1s and N1s) of untreated and treated PET braids

Table 2. Binding energy [eV] and atomic concentration [%] of the chemical bonds identified in the XPS spectra for PET fibers.

Chemical bond	PET	PET_NH ₃	PET_O ₂ EDA
C1s			
C–C	284.6	284.6	284.7
C=C	68.9%	59.3%	63.3%
C–O	286.0	285.9	286.1
C–N	23.5%	32.8%	29.8%
C=N			
O–C=O	288.7	288.6	288.9
N–C=O	7.5%	7.9%	6.9%
O1s			
NH _x –C=O	—	530.4	530.8
		51.4%	69.9%
C=O	532.0	531.3	532.2
N–C=O	60%	34.6%	9.5%
C–O	533.3	532.5	532.9
C–O–C	40%	14.0%	20.6%
O–C–O			
N1s			
C–NH ₂	—	398.4	398.3
		91.4%	89.7%
C–NHR	—	400.2	399.0
C=N		8.6%	10.3%
C–NH ₃ ⁺			

The carbon atoms on the benzene ring, the methylene carbon singly linked to an oxygen atom, and the ester carbon atoms were all identified as peaks in the C1s high-resolution spectra for all

PET samples.^[24,29,30] For both treated samples, a slight change in the shape of the curve between 286 and 289 eV is observed, which could be due to the contribution of new functionalities involving nitrogen species.^[24,28] PET's O1s spectrum can be divided into two peaks, one for oxygen atoms linked to one carbon atom and the other for oxygen atoms bonded to two carbon atoms.^[24] In the functionalized PET samples, a new peak appears in the O1s spectrum, which could be attributed to amide groups (NH_x–C=O).^[24] The N1s peak of both treated samples could be resolved into two peaks. In both cases, endowing the braids with amines was accomplished, as seen in the presence of primary amines binding energies (C–NH₂ and C–NH₃⁺). However, when comparing the different treatments on PET, it is important to mention that the NH₃ plasma displayed a higher atomic concentration of nitrogen, resulting from nitrogen-containing functional groups (mainly primary amines).

The chemical bonds and binding energy (eV) of PLA samples, along with atomic concentration, are shown in **Table 3**. **Figure 6** shows the survey spectra of the PLA surface before and after both treatments, along with the C1s (Figure 6a) and O1s and N1s high-resolution spectra (Figure 6b).

The C1s spectra of PLA were deconvoluted into three peaks: 285 eV, which may be attributed to C–C and C–H bonds, 286.6 eV (C–O), and 289.3 eV (O=C–O).^[31–33] After NH₃ plasma and O₂ EDA treatment, the characteristic peaks of PLA are still visible, with slight energy shifts and different peak widths, due to the evident incorporation of nitrogen on the PLA surface. The O1s spectrum of PLA untreated and treated samples can be decomposed into two peaks, attributed to the C–O and C=O bonds.^[34,35] The N1s spectrum of both samples could be decomposed into two, assigned to imine groups (C=N) and amine groups (C–N).^[36] However, the O₂ EDA treatment yielded a much higher concentration

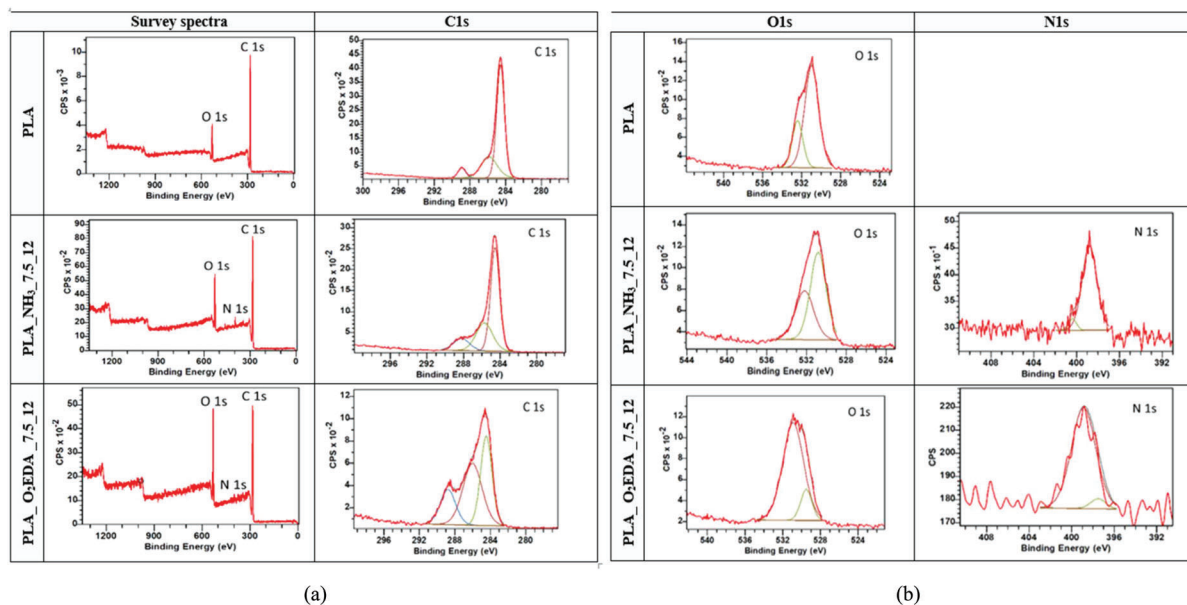


Figure 6. a) XPS overview and detailed spectra (C1s) of untreated and treated PLA braids, b) detailed spectra (O1s and N1s) of untreated and treated PLA braids.

Table 3. Binding energy (eV) and atomic concentration (%) of the chemical bonds identified in the XPS spectra for PLA fibers.

Chemical bond	PLA	PLA_NH ₃	PLA_O ₂ EDA
C1s			
C–C	284.6	284.6	284.5
C–H	68.0%	58.5%	37.1%
C–O	285.9	285.7	286.0
C–NH ₂	26.0%	29.2%	43.4%
O–C=O	288.9	288.2	288.8
C=O	6.0%	12.3%	19.5%
O1s			
C–O	531.0	530.8	529.5
	74.4%	60.7%	14.7%
C=O	532.4	532.2	530.9
	60%	39.3%	85.3%
N1s			
C=N	—	398.8	397.5
		93.3%	5.9%
C–N	—	400.4	398.9
		6.7%	94.1%

of amines when compared with PLA_NH₃ plasma-treated samples, which corroborates the results obtained in the Orange II method and by fuchsin acid dye. In all treated samples (for both PET and PLA braids), there was a clear indication of the effective functionalization with amine groups.

Possible morphological changes in the functionalized braids were studied by SEM, and the images are presented in **Figure 7**.

The PET filaments seemed smooth, with minor imperfections on the surface, while plasma treatment influenced their morphology. The sample treated with NH₃ plasma still shows a smooth

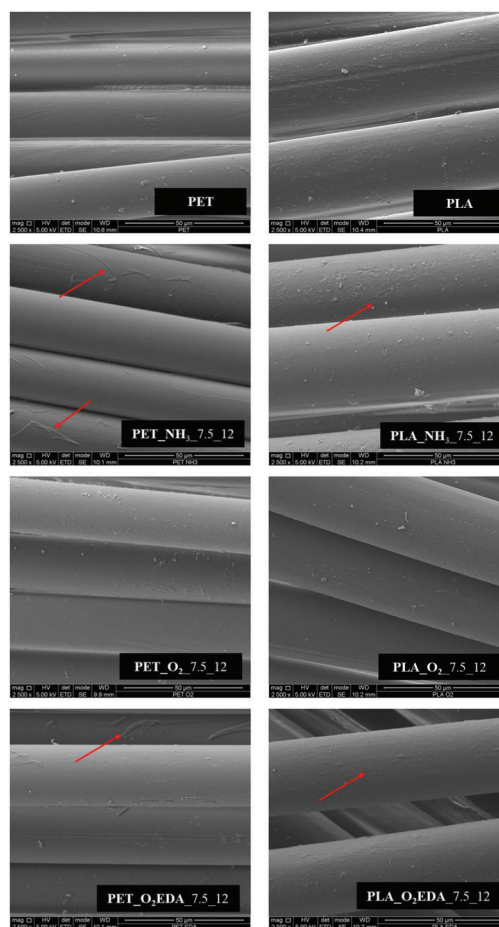


Figure 7. Scanning electron microscopy (SEM) images of untreated and treated PET and PLA braids.

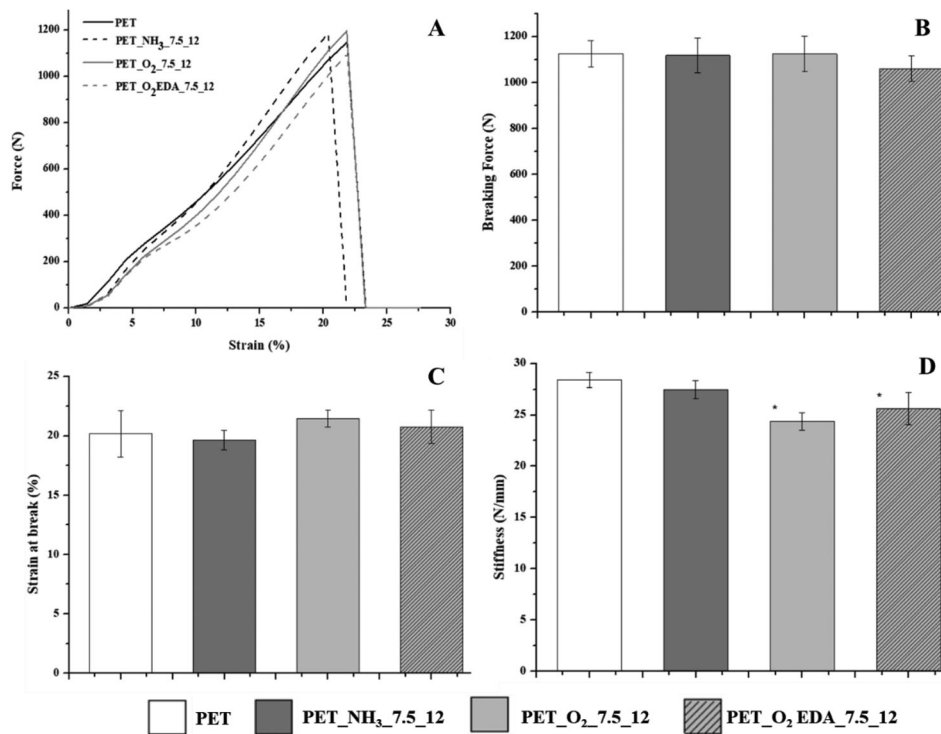


Figure 8. a) Force/strain representative curves of the functionalized PET braids, b) breaking force (N), c) strain at break (%), and d) stiffness (N mm^{-1}) ($* p < 0.05$).

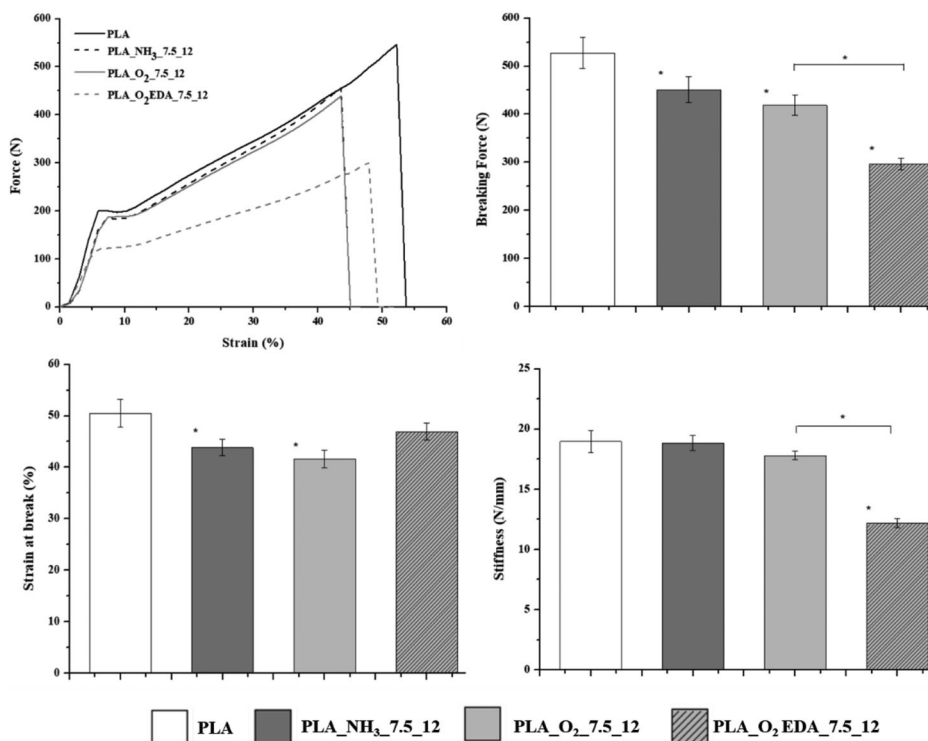


Figure 9. a) Force/strain representative curves of the functionalized PLA braids, b) breaking force (N), c) strain at break (%), and d) stiffness (N mm^{-1}) ($* p < 0.05$).

surface but it is possible to observe surface peeling in some areas. After O₂ plasma, the filaments' surface became more irregular and rough, which may be attributed to etching. Some surface peeling on PET samples treated with O₂ plasma and EDA immersion is also observed. Although some impurities are also observed in PLA filaments, surface roughening due to the abrasive effect of the functionalization is evident on NH₃ plasma treated samples and on the O₂-EDA treated samples. Plasma carries activated species such as electrons, radicals, ions, and photons, which can start reactions on polymeric surfaces. These reactions include the insertion of additional functional groups to polymer surfaces as a result of recombination of radicals generated on the polymer surfaces with activated species in the plasma but also includes surface etching reactions, which are caused by high-energy particles bombarding the fiber surface during the discharge, leading to the changes in the polymer surface.^[37] Nevertheless, the changes observed did not significantly alter surface morphology.

Tensile testing was performed to assess the eventual effect of the plasma treatment on the tensile performance of the PET and PLA braids. Mechanical properties of modified and unmodified PET were compared by tensile testing (Figure 8). The results show that PET braids modified by both plasma treatments and immersion in EDA solution exhibit tensile properties comparable to unmodified PET; so, fiber integrity was maintained. In contrast, the results shown in Figure 9 for PLA confirm a significant loss of tensile properties for both treatments. The breaking force of PLA decreased from 527.3 N to 451.3 N (≈14% decrease) for the NH₃ treated sample. The breaking force of the O₂ treated braid was statistically similar to the previous. However, after immersion in EDA, it further decreased to 296.4 N (≈44% decrease). No statistical differences were found between the stiffness of PLA and PLA modified with both plasma treatments. However, a significant decrease from 19.0 to 12.2 N mm⁻¹ (≈36% decrease) was found for the O₂ sample immersed in EDA.

Polyethylene terephthalate (PET) is a polymer broadly used in numerous industries due to its desirable bulk properties, high strength, and thermal resistance.^[37,38] Nevertheless, there are reports of tensile strength decrease of PET after treatment with EDA.^[39,40] These findings led to the conclusion that the plasma process parameters (time, plasma pressure) and EDA immersion parameters were adequate for minimizing severe damaging events that could damage the PET braids while permitting the absorption of amine groups. On the other hand, PLA is a heat sensitive polymer and may exhibit a reduction of properties related to thermal deterioration.^[41] Thus, although functionalization occurred, the heat generated during NH₃ and O₂ plasma treatments may have led to PLA damage to some extent and, consequently, changes in their mechanical strength. However, these changes were even more pronounced after immersion in a heated water-based EDA solution, which may be attributed to hydrolysis. It is known that the primary factor of PLA degradation is hydrolysis, which is influenced by temperature conditions and results in the weakening of mechanical properties.^[42] Nevertheless, as already shown in a previous work,^[8,9] PET yarns are the primary providers of tensile strength for the produced hybrid braids and, consequently, for the final medical device. As such, the mechanical properties of the previously optimized hybrid braids are main-

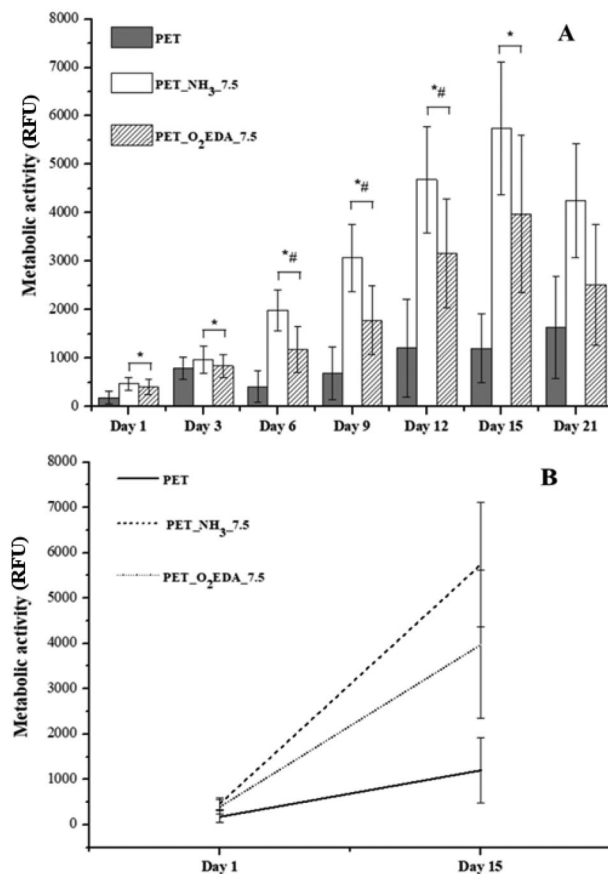


Figure 10. a) Metabolic activity of fibroblast cells on PET braids, measured up to 21 days by resazurin assay. * $p < 0.05$, significant differences from PET, for each time-point. # $p < 0.05$, significant differences of EDA from NH₃, for each time-point. b) Growth rate comparing Day 1 to Day 15.

tained after both treatments and can still fulfill the high mechanical demands of tissues such as tendons or ligaments.

3.2. In Vitro Biological Characterization

Cell culture assays were performed on PET samples (PET, PET_NH₃_7.5_12, and PET_O₂_EDA_7.5_12) to elucidate the impact of the surface treatments on cell adhesion and proliferation.

The metabolic activity of cells seeded on the materials was analyzed and compared by the resazurin assay over the experiment at different time points. As observed in Figure 10a, all treated samples display increased cellular metabolic activity until day 15, with higher values than untreated PET. However, it could be observed that cell growth was faster for the NH₃ treated braids (Figure 10b) between day 6 and day 12 of the experiment ($p < 0.05$). No statistical difference was observed between both treatments on day 15.

Fibroblasts adherence and morphology were assessed by SEM (Figure 11). However, few cells were present on the surface of the materials, meaning that the vast majority of cells, which are metabolically active, as seen in Figure 10, migrated to the core of the braids after seeding. This effect is beneficial, taking into

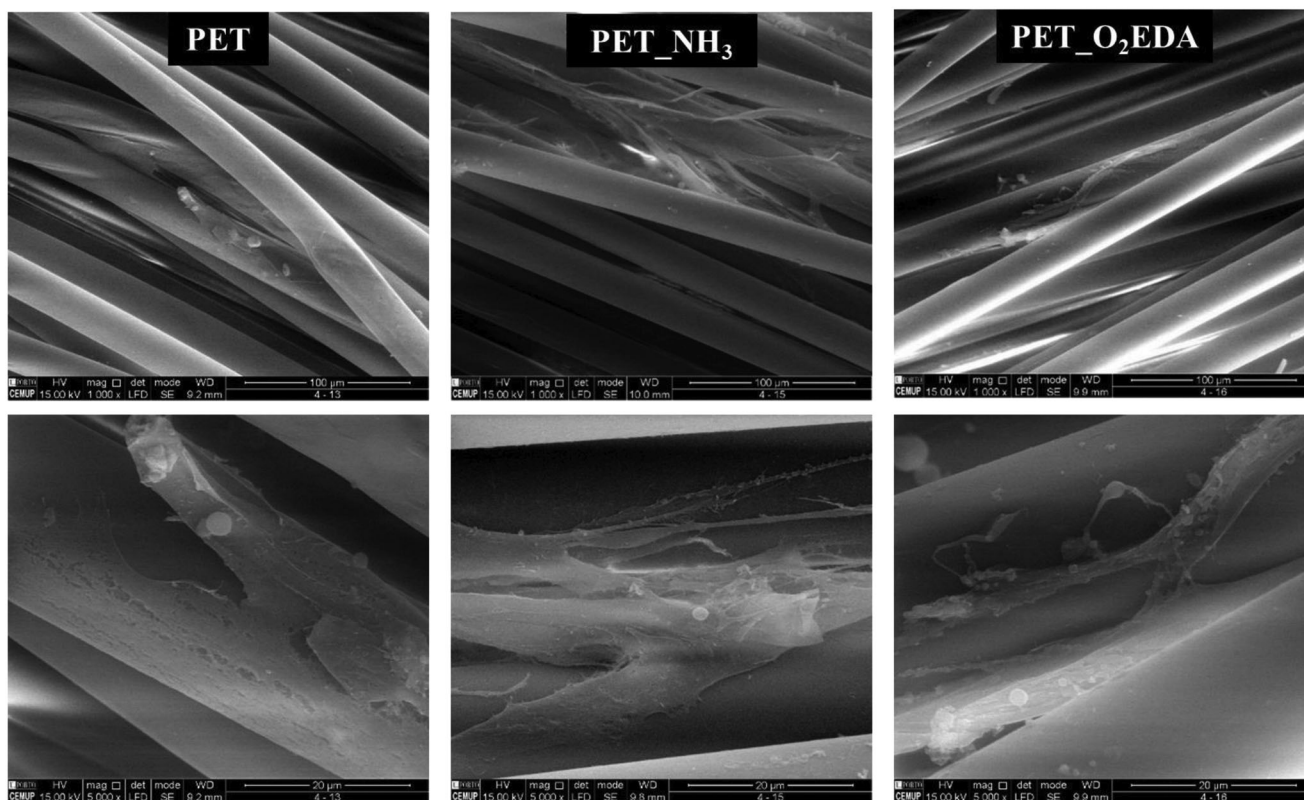


Figure 11. SEM images of cell adhesion in PET braids treated with NH_3 plasma and O_2 plasma followed by immersion in EDA, day 15 of the experiment, at 1000 \times and 5000 \times .

account the application of the proposed medical device, where tissue ingrowth into the structure is fundamental for an effective biointegration of the device.

Nevertheless, the morphology of the few fibroblasts visible on each sample's surface varied in accordance with the type of surface treatment. The cells seeded on the untreated PET fibers displayed adhesion but could not expand the cytoplasm, preventing proliferation and interaction with adjacent fibers. However, the cells seeded on the O_2 /EDA treated fibers displayed an extended morphology with a somewhat restricted interaction with the surrounding fibers. The cell morphology adhering to the NH_3 plasma-treated samples displayed cytoplasmic spreading with visible filopodia to the surrounding fibers, meaning that there was strong adhesion to the material, the cells were well-adapted to the material topography, and that there was good interaction within the fibers.

The hydrophobic/hydrophilic balance, electrostatic interactions, chemical functioning, and biological signals of bio-material surfaces can influence cell adhesion.^[28] Primary amine functional groups can aid the covalent immobilization of biomolecules such as RGD tripeptide binding sites or collagen.^[43] Furthermore, at physiological pH, protonated amines can introduce a localized positive charge in an aqueous solution, which can be employed for electrostatic interactions with the negatively-charged surfaces of cells and proteins, promoting cell adhesion and proliferation as well as long-term survivability.^[44]

4. Conclusion

Both surface treatments were effective for incorporating primary amine groups on the surfaces of both PET and PLA. The chosen treatment parameters allowed an efficient amine group grafting level without compromising the topography and mechanical properties of the hybrid braids. The NH_3 treatment resulted in a higher presence of primary amines with increased cell–braid interaction, enhancing cell adhesion and proliferation, which was confirmed by the resazurin experiment and SEM analysis. On top of these results, this approach is also faster, can be more easily scaled up, and is more environmentally friendly than O_2 /EDA treatment, showing potential for application in the final hybrid medical device. As one of the major reasons for the long-term failure of commercially available synthetic devices is the lack of host tissue integration, the presented functionalization will potentially enhance rapid cell migration and adhesion to the scaffold after its clinical application. This is expected to help posterior cell differentiation to assure the integration of the scaffold with the native tissues in the long-term.

Acknowledgements

T.P. and D.S. contributed equally to this work. Financial support from PT national funds (FCT/MCTES, Fundação para a Ciência e Tecnologia and Ministério da Ciência, Tecnologia e Ensino Superior) through the project UIDB/50006/2020 is acknowledged by REQUIMTE-LAQV authors. IPC

authors acknowledge “National Funds through FCT—Portuguese Foundation for Science and Technology,” References UIDB/05256/2020 and UIDP/05256/2020. T.P. acknowledges the financial support from FCT and ESF (European Social Fund) through North Portugal Regional Operational Program, through the PhD Grant PD/BD/143035/2018.

Conflict of Interest

The authors declare no conflict of interest.

Data Availability Statement

The data that support the findings of this study are available from the corresponding author upon reasonable request.

Keywords

ethylenediamine, hybrid medical device (PET/PLA), NH₃ plasma, surface functionalization, tissue repair

Received: June 24, 2022

Revised: September 29, 2022

Published online:

- [1] J. Hou, R. Yang, I. Vuong, F. Li, J. Kong, H. -Q. Mao, *Acta Biomater.* **2021**, *130*, 1.
- [2] J. Brebels, A. Mignon, *Polymers* **2022**, *14*, 867.
- [3] E. Bianchi, M. Ruggeri, S. Rossi, B. Vigani, D. Miele, M. C. Bonferoni, G. Sandri, F. Ferrari, *Pharmaceutics* **2021**, *13*, 89.
- [4] M. N. Hafeez, N. d'Avanzo, V. Russo, L. Di Marzio, F. Cilurzo, D. Paolino, M. Fresta, B. Barboni, H. A. Santos, C. Celia, *Stem Cells Int.* **2021**, *2021*, 1488829.
- [5] Y. J. No, M. Castilho, Y. Ramaswamy, H. Zreiqat, *Adv. Mater.* **2020**, *32*, 1904511.
- [6] B. Bauer, C. Emonts, L. Bonten, R. Annan, F. Merkord, T. Vad, A. Idrissi, T. Gries, A. Blaeser, *Fibers* **2022**, *10*, 23.
- [7] M. Kun, C. Chan, S. Ramakrishna, A. Kulkarni, K. Vadodaria, in *Advanced Textiles for Wound Care*, Elsevier; **2019**. pp. 329–62.
- [8] T. Peixoto, S. Carneiro, R. Fangueiro, R. M. Guedes, M. C. Paiva, M. A. Lopes, *J. Appl. Polym. Sci.* **2022**, *139*, 52013.
- [9] T. Peixoto, S. Carneiro, F. Pereira, C. Santos, R. Fangueiro, I. Duarte, M. C. Paiva, M. A. Lopes, R. M. Guedes, *Polym. Adv. Technol.* **2022**, *33*, 2362.
- [10] D. S. Morais, J. Torres, R. M. Guedes, M. A. Lopes, *Ann. Biomed. Eng.* **2015**, *43*, 2025.
- [11] J. S. Bergström, D. Hayman, *Ann. Biomed. Eng.* **2016**, *44*, 330.
- [12] J. Leyden, Y. Kaizawa, J. Chang, in *Regenerative Medicine and Plastic Surgery*, Springer; **2019**. pp. 355–67.
- [13] N. Eswaramoorthy, D. R. Mckenzie, *Biophys. Rev.* **2017**, *9*, 895.
- [14] A. R. Shirvan, A. Nouri, *Adv. Funct. Prot. Text* **2020**, 291.
- [15] L. Minati, C. Migliaresi, L. Lunelli, G. Viero, M. Dalla Serra, G. Speranza, *Biophys. Chem.* **2017**, *229*, 151.
- [16] C. I. L. Justino, A. C. Duarte, T. A. P. Rocha-Santos, *TrAC, Trends Anal. Chem.* **2016**, *85*, 36.
- [17] M. Aflori, M. Drobotă, D. G. Dimitriu, I. Stoica, B. Simionescu, V. Harabagiu, *Mater. Sci. Eng., B* **2013**, *178*, 1303.
- [18] M. Domingos, F. Intranuovo, A. Gloria, R. Cristina, L. Ambrosio, P. J. Bártolo, P. Favia, *Acta Biomater.* **2013**, *9*, 5997.
- [19] Q. Cheng, B. Li-P. Lee, K. Komvopoulos, Z. Yan, S. Li, *Tissue Eng., Part A* **2013**, *19*, 1188.
- [20] R. Ghoheira, N. De Geyter, R. Morent, Plasma surface functionalization of biodegradable electrospun scaffolds for tissue engineering applications. *Biograd Polym Recent Dev New Perspect Geraldine, RC*, Ed. **2017**, pp. 191–236.
- [21] Ž. Marjanović-Balaban, D. Jelić, In: *Biomaterials in Clinical Practice*, Springer; **2018**. pp. 101–17.
- [22] W. Khan, E. Muntimadugu, M. Jaffe, A. J. Domb, In: *Focal controlled drug delivery*, Springer; **2014**. pp. 33–59.
- [23] M. Asadian, H. Declercq, M. Cornelissen, R. Morent, N. De Geyter, in: *31st International conference on surface modification technologies*. **2017**.
- [24] J. Casimiro, B. Lepoittevin, C. Boisse-Laporte, M. G. Barthés-Labrousse, P. Jegou, F. Brisset, P. Roger, *Plasma Chem. Plasma Process.* **2012**, *32*, 305.
- [25] Y. Avny, L. Rebenfeld, *J. Appl. Polym. Sci.* **1986**, *32*, 4009.
- [26] S. Noel, B. Liberelle, L. Robitaille, G. De Crescenzo, *Bioconjugate Chem.* **2011**, *22*, 1690.
- [27] P. Hamerli, *Biomaterials* **2003**, *24*, 3989.
- [28] Z. Zheng, L. Ren, W. Feng, Z. Zhai, Y. Wang, *Appl. Surf. Sci.* **2012**, *258*, 7207.
- [29] Z. Zheng, L. Ren, Z. Zhai, Y. Wang, F. Hang, *Mater. Sci. Eng., C* **2013**, *33*, 3041.
- [30] E. Rodră-Guez-Alba, N. Dionisio, M. Pérez-Calixto, L. Huerta, L. García-Uriostegui, M. Hautefeuille, G. Vázquez-Victorio, G. Burillo, *Radiat. Phys. Chem.* **2020**, *176*, 109070.
- [31] Yi-W. Yang, J. -Y. Wu, C. -C. Liao, K. -Y. Cheng, M. -H. Chiang, J. -S. Wu, *Plasma Processes Polym.* **2015**, *12*, 678.
- [32] J. Yang, J. Bei, S. Wang, *Biomaterials* **2002**, *23*, 2607.
- [33] Yu Ren, L. Xu, C. Wang, X. Wang, Z. Ding, Y. Chen, *Appl. Surf. Sci.* **2017**, *426*, 612.
- [34] A. Davoodi, H. H. Zadeh, M. D. Joupari, M. A. Sahebalzamani, M. R. Khani, S. Shahabi, *AIP Adv.* **2020**, *10*, 125205.
- [35] J. i. E. Song, W. S. Song, S. Y. Yeo, H. R. Kim, S. o. H. Lee, *Text. Res. J.* **2017**, *87*, 1177.
- [36] S. Sarapirom, L. D. Yu, D. Boonyawan, C. Chaiwong, *Appl. Surf. Sci.* **2014**, *310*, 42.
- [37] N. Inagaki, K. Narushim, N. Tuchida, K. Miyazaki, *J. Polym. Sci., Part B: Polym. Phys.* **2004**, *42*, 3727.
- [38] A. M. Grumezescu, A. E. Stoica, M.-S. Dima-Bălcescu, C. Chircov, S. Gharbia, C. Baltă, M. Rosu, H. Herman, A. M. Holban, A. Fica, B. S. Vasile, E. Andronescu, M. C. Chifriuc, A. Hermenean, *J Clin Med* **2019**, *8*, 1039.
- [39] V. Muthuvijayan, J. Gu, R. S. Lewis, *Acta Biomater.* **2009**, *5*, 3382.
- [40] D. Morais, M. Rodrigues, C. j. U. Lopes, F. Vaz, L. Grenho, M. Fernandes, R. Guedes, M. Lopes, *J. Biomed. Mater. Res., Part B* **2021**, *109*, 2213.
- [41] V. Taubner, R. Shishoo, *J. Appl. Polym. Sci.* **2001**, *79*, 2128.
- [42] S. Khalaj Amnieh, P. Mosaddegh, M. Mashayekhi, M. Kharaziha, *J. Appl. Polym. Sci.* **2021**, *138*, 50389.
- [43] Z. i. X. Xu, T. Li, Z. -M. Zhong, D. -S. Zha, S. -H. Wu, F. u. Q. Liu, W. -D. e. Xiao, X. -R. Jiang, X. -X. Zhang, J. -T. Chen, *Biopolymers* **2011**, *95*, 682.
- [44] G. Aziz, N. De Geyter, R. Morent, *Adv. Bioeng.* **2015**, 21.